Neutrino mass model at a three-loop level from a non-holomorphic modular A_4 symmetry*

Takaaki Nomura[1†] Hiroshi Okada[2‡]

[1]College of Physics, Sichuan University, Chengdu 610065, China
[2]Department of Physics, Henan Normal University, Xinxiang 453007, China

Abstract: We study a three-loop induced neutrino mass scenario from a non-holomorphic modular A_4 flavor symmetry and obtain the minimum scenario leading to predictions of the lepton masses, mixing angles, and Dirac and Majorana phases, which are shown through chi square analyses. In addition, we discuss the lepton flavor violations, muon anomalous magnetic moment, lepton universality, and relic density of the dark matter candidate. Moreover, we show that our model can be extended to satisfy the observed relic density of dark matter within the limit of perturbation by adding one singlet scalar boson without changing predictions in the neutrino sector.

Keywords: radiative neutrino mass generation, neutrino mass matrix, modular flavor symmetry, phenomenological model building

DOI: 10.1088/1674-1137/ae15ee **CSTR:** 32044.14.ChinesePhysicsC.50023108

I. INTRODUCTION

The successful construction of the non-holomorphic modular symmetry framework by Qu and Ding [1] has enabled us to safely handle the beyond the standard model (BSM) without super-symmetric theories when using the framework for a flavor symmetry. In fact, the non-holomorphic symmetries have been applied to some non-supersymmetric models [2−12] in order to restrict the number of model parameters. In constructing a model, we have the advantage of applying non-supersymmetric framework to reduce the number of new fields when extra fields are required to cancel a gauge anomaly in the supersymmetric case.

Radiatively induced neutrino mass models are representative scenarios that do not require the super-symmetric framework, and new particles can be connected to the standard model particles. Sometimes, the model can possess a dark matter (DM) candidate [13] that often requires an additional symmetry to stabilize it. Thus, constructing radiative neutrino mass models (with DM) using the non-holomorphic modular symmetry can make a model more attractive by realizing more predictability.

In this study, we apply a non-holomorphic A_4 flavor symmetry to a well-known three-loop neutrino mass model [14]. The three-loop neutrino model is phenomenologically interesting, as the scale of new particles would be smaller compared to lower loop (or tree) level models owing to loop suppression. We then expect rich phenomenology such as collider and lepton flavor physics. The non-holomorphic modular symmetry framework is suitable for constructing such a three-loop model in a minimal manner; if we consider a holomorphic framework, we need to add more fields to cancel the gauge anomaly. Then, we need to determine the minimal number of free parameters to fit the observables in the lepton sector under the non-holomorphic modular A_4 symmetry. Through chi-square numerical analysis, we search for the minimum model to predict the lepton masses and mixing angles in addition to reproducing the current neutrino observables in Nufit 6.0 [15]. Then, we perform further numerical analyses to satisfy lepton flavor violations (LFVs), the muon anomalous magnetic moment, (muon $g-2$), lepton universality, and DM. The results show that relic density is too large within the limit of perturbation, thereby requiring a new interaction that adds one singlet scalar boson without changing predictions in the neutrino sector.

This paper is organized as follows. In Sec. II, we ex-

Received 17 July 2025; Accepted 21 October 2025; Published online 22 October 2025

* Takaaki Nomura is supported by the Fundamental Research Funds for the Central Universities. Hiroshi Okada is supported by Zhongyuan Talent (Talent Recruitment Series) Foreign Experts Project

† E-mail: nomura@scu.edu.cn
‡ E-mail: hiroshi3okada@htu.edu.cn

plain our minimum three-loop neutrino mass model and construct the renormalizable Lagrangian in the lepton sector, Higgs sector, charged-lepton sector, heavier Majorana fermion sector, and active-neutrino sector. Then, we formulate the LFVs, muon $g-2$, lepton universality, and relic density of the DM. In Sec. III, we perform χ square analysis and present predictions for normal and inverted hierarchies in the neutrino sector. By employing the benchmark points of the best-fit values in the lepton sector, we further demonstrate the numerical analyses for the LFVs, muon $g-2$, lepton universality, and relic density of the DM. We present the conclusions and discussion in Sec. IV. In Appendix A, we show the three-loop function in the neutrino sector.

II. MODEL SETUP

In this section, we show the setup of the model based on a $G_{\rm SM}\times A_4$ symmetry, where $G_{\rm SM}$ is the SM gauge symmetry and A_4 is the modular one. In the lepton sector, we introduce a singlet fermion, which is a triplet under A_4 with modular weight 0. In the scalar sector, we introduce two charged singlets distinguished by modular weights +2 and –1. The SM leptons $\overline{L_L}$ and ℓ_R are also A_4 triplets with modular weights –1 and +1, respectively. The assignments are summarized in Table 1. By assigning modular weights, we can eliminate unwanted terms such as $\overline{N_R}L_L H$, and the neutrino masses are generated at the three-loop level, as discussed below.

The relevant Lagrangian under these symmetries is given by

$$\begin{aligned}-\mathcal{L}_\ell =& a_e\left[y_1\overline{L_{L_e}}+y_2\overline{L_{L_\tau}}+y_3\overline{L_{L_\mu}}\right]e_R H\\ &+a_\mu\left[y_2\overline{L_{L_\mu}}+y_3\overline{L_{L_e}}+y_1\overline{L_{L_\tau}}\right]\mu_R H\\ &+a_\tau\left[y_3\overline{L_{L_\tau}}+y_1\overline{L_{L_\mu}}+y_2\overline{L_{L_e}}\right]\tau_R H\\ &+a_\nu\Big[y_1(\overline{L_{L_\mu}}\cdot L^C_{L_\tau}-\overline{L_{L_\tau}}\cdot L^C_{L_\mu})+y_2(\overline{L_{L_\tau}}\cdot L^C_{L_e}-\overline{L_{L_e}}\cdot L^C_{L_\tau})\\ &+y_3(\overline{L_{L_e}}\cdot L^C_{L_\mu}-\overline{L_{L_\mu}}\cdot L^C_{L_e})\Big]S_1^- + b_\nu\overline{e^C_R}[y_1N_{R_1}+y_2N_{R_3}\\ &+y_3N_{R_2}]S_2^+ + c_\nu\overline{\mu^C_R}\left[y_2N_{R_2}+y_3N_{R_1}+y_1N_{R_3}\right]S_2^+\\ &+d_\nu\overline{\tau^C_R}\left[y_3N_{R_3}+y_1N_{R_2}+y_2N_{R_1}\right]S_2^+\\ &+M_1(\overline{N^C_{R_1}}N_{R_1}+\overline{N^C_{R_2}}N_{R_3}+\overline{N^C_{R_3}}N_{R_2})\\ &M_2\Big[y_1(2\overline{N^C_{R_1}}N_{R_1}-\overline{N^C_{R_2}}N_{R_3}-\overline{N^C_{R_3}}N_{R_2})\\ &+y_2(2\overline{N^C_{R_2}}N_{R_2}-\overline{N^C_{R_1}}N_{R_3}-\overline{N^C_{R_3}}N_{R_1})\\ &+y_3(2\overline{N^C_{R_3}}N_{R_3}-\overline{N^C_{R_1}}N_{R_2}-\overline{N^C_{R_2}}N_{R_1})\Big]+\text{h.c.},\end{aligned} \tag{1}$$

where we define $Y_3^{(0)}=[y_1,y_2,y_3]$ [1], and "$\cdot$" indicates the $i\sigma_2$ factor that makes the term $SU(2)_L$ invariant. The first two terms generate the mass of the charged leptons, and parameters $\{a_e,a_\mu,a_\tau\}$ are real without loss of generality and are rephased into e_R,μ_R,τ_R, respectively.

Table 1. Field contents and their charge assignments in the model under $SU(2)_L\times U(1)_Y\times A_4$, where $-k_I$ is the number of the modular weight. Here, {1} represents the combination of A_4 singlets $\{1,1',1''\}$.

	Leptons			Bosons		
	$\overline{L_L}$	ℓ_R	N_R	H	S_1^+	S_2^+
$SU(2)_L$	**2**	**1**	**1**	**2**	**1**	**1**
$U(1)_Y$	$-\frac{1}{2}$	1	0	$\frac{1}{2}$	+1	+1
A_4	3	{1}	3	1	1	1
$-k_I$	–1	+1	0	0	+2	–1

A. Scalar sector

The scalar potential in the model is given by

$$\begin{aligned}\mathcal{V} =& \mu_H^2|H|^2+\mu_{S_1}^2|S_1^+|^2+\mu_{S_2}^2|S_2^+|^2+\lambda_0[(S_1^+S_2^-)^2+\text{h.c.}]\\ &+\lambda_H|H|^4+\lambda_{S_1}|S_1^+|^4+\lambda_{S_2}|S_2^+|^4+\lambda_{HS_1}|H|^2|S_1^+|^2\\ &+\lambda_{HS_2}|H|^2|S_2^+|^2+\lambda_{S_1S_2}|S_1^+|^2|S_2^+|^2.\end{aligned} \tag{2}$$

The SM Higgs field is denoted by

$$H=\begin{pmatrix} w^+\\ \dfrac{v+\tilde{h}+iz}{\sqrt{2}}\end{pmatrix}, \tag{3}$$

and $v\approx 246$ GeV is the vacuum expectation value (VEV) in the Higgs basis after the spontaneous symmetry breaking, z is absorbed by the neutral gauge boson of the SM Z, and w^+ is absorbed by the charged gauge boson of the SM W^+. The charged scalar masses are given by

$$m_{S_1}^2=\mu_{S_1}^2+\frac{1}{2}\lambda_{HS_1}v^2, \tag{4}$$

$$m_{S_2}^2=\mu_{S_2}^2+\frac{1}{2}\lambda_{HS_2}v^2. \tag{5}$$

In the numerical analysis, we consider $m_{S_{1,2}}$ to be free parameters.

B. Charged-lepton mass matrix

After the spontaneous electroweak symmetry breaking, the charged-lepton mass matrix M_e is given by

$$M_e=\frac{v}{\sqrt{2}}\begin{pmatrix} y_1 & y_3 & y_2\\ y_3 & y_2 & y_1\\ y_2 & y_1 & y_3\end{pmatrix}\begin{pmatrix} a_e & 0 & 0\\ 0 & a_\mu & 0\\ 0 & 0 & a_\tau\end{pmatrix}. \tag{6}$$

Then, the charged-lepton mass matrix is diagonalized by a bi-unitary mixing matrix as $D_\ell \equiv \text{diag}(m_e, m_\mu, m_\tau) = V_{eL}^\dagger M_e V_{eR}$. Therefore, $\ell_{L(R)} \equiv V_{eL(R)} \ell'_{L(R)}$, where $\ell'_{L(R)}$ is the mass eigenstate. These three parameters are used to fit the mass eigenvalues of charged-leptons by solving the following three relations:

$$\text{Tr}[M_e M_e^\dagger] = |m_e|^2 + |m_\mu|^2 + |m_\tau|^2, \tag{7}$$

$$\text{Det}[M_e M_e^\dagger] = |m_e|^2 |m_\mu|^2 |m_\tau|^2, \tag{8}$$

$$\begin{aligned}&(\text{Tr}[M_e M_e^\dagger])^2 - \text{Tr}[(M_e M_e^\dagger)^2] \\ &= 2(|m_e|^2|m_\mu|^2 + |m_\mu|^2|m_\tau|^2 + |m_e|^2|m_\tau|^2).\end{aligned} \tag{9}$$

For convenience in constructing the neutrino-mass matrix, we define $\tilde{D}_\ell$, which is given by $D_\ell \equiv m_\tau \tilde{D}_\ell$.

C. Heavier Majorana fermion-mass matrix

The heavier Majorana mass matrix is given by

$$M_N = M_1 \left[\begin{pmatrix} 1 & 0 & 0 \\ 0 & 0 & 1 \\ 0 & 1 & 0 \end{pmatrix} + \tilde{M}_2 \begin{pmatrix} 2y_1 & -y_3 & -y_2 \\ -y_3 & 2y_2 & -y_1 \\ -y_2 & -y_1 & 2y_3 \end{pmatrix} \right] \equiv M_1 \tilde{M}_N, \tag{10}$$

where $\tilde{M}_2 \equiv M_2/M_1$ can be real without loss of generality. M_N is diagonalized by $D_N \equiv U_N^T M_N U_N$ ($\tilde{D}_N \equiv U_N^T \tilde{M}_N U_N$); therefore, $N_R \equiv U_N \psi_R$. Here, ψ_R is the mass eigenstate.

D. Active neutrino-mass matrix

The active neutrino mass matrix is given at the three-loop level via the following Lagrangian in terms of the mass eigenstates:

$$a_\nu \left(\overline{\nu_L} H \ell'^C_L + \overline{\ell'_L} H^T \nu^C_L \right) S_1^- + b_\nu \overline{\ell'^C_R} Y \psi_R S_2^+ + \text{h.c.}, \tag{11}$$

where $H \equiv h V_{eL}^*$ and $Y \equiv V_{eR}^T y U_N$. The Yukawa matrices y and h are as follows:

$$h = \begin{pmatrix} 0 & y_3 & -y_2 \\ -y_3 & 0 & y_1 \\ y_2 & -y_1 & 0 \end{pmatrix}, \tag{12}$$

$$y = \begin{pmatrix} 1 & 0 & 0 \\ 0 & \tilde{c}_\nu & 0 \\ 0 & 0 & \tilde{d}_\nu \end{pmatrix} \begin{pmatrix} y_1 & y_3 & y_2 \\ y_3 & y_2 & y_1 \\ y_2 & y_1 & y_3 \end{pmatrix}, \tag{13}$$

where $\tilde{c}(\tilde{d})_\nu \equiv c(d)_\nu / b_\nu$ are complex free parameters. The neutrino mass matrix is then given by

$$(m_\nu)_{ij} \approx -\frac{\lambda_0 (a_\nu b_\nu)^2}{(4\pi)^6} \frac{m_\tau^2}{M_1} H^* \tilde{D}_\ell Y^* \tilde{D}_N F Y^\dagger \tilde{D}_\ell H^\dagger \equiv \kappa \tilde{m}_\nu, \tag{14}$$

Here, F is a loop function via three loop diagram and it depends on the mass eigenvalues of $\{\psi_R, S_1^+, S_2^+\}$. [1] Since the masses of ψ_R contribute to the structure of neutrino mass matrix, there would be too many free parameters to get some predictions for the neutrino sector. Thus, we consider a special situation among the mass hierarchies of ψ_R, S_1^+, S_2^+ so that F is independent of the structure of neutrino mass matrix. When we assume $D_{N_i} \ll m_{S_1} \sim m_{S_2}$, one finds that the dominant part of the loop-function F is a constant and can explicitly be given by $F \approx 0.062$. In detail, one finds Appendix A. Thus, we redefine the neutrino mass matrix as follows:

$$\kappa \equiv -\frac{\lambda_0 F (a_\nu b_\nu)^2}{(4\pi)^6} \frac{m_\tau^2}{M_1}, \tag{15}$$

$$\tilde{m}_\nu \equiv H^* \tilde{D}_\ell Y^* \tilde{D}_N Y^\dagger \tilde{D}_\ell H^\dagger. \tag{16}$$

The dimensionless matrix $\tilde{m}_\nu$ is diagonalized by a unitary matrix U_ν as $U_\nu^T \tilde{m}_\nu U_\nu = \tilde{D}_\nu$, where $\tilde{D}_\nu = \text{diag}[\tilde{D}_{\nu_1}, \tilde{D}_{\nu_2}, \tilde{D}_{\nu_3}]$, and the Pontecorvo-Maki-Nakagawa-Sakata unitary matrix U_{PMNS} is defined by $V_{eL}^\dagger U_\nu$. Note here that the lightest neutrino mass is zero due to the two-matrix rank of the neutrino. Thus, the atmospheric mass squared difference Δm^2_{atm} is as follows:

$$\text{NH}: \ \Delta m^2_{atm} = \kappa^2 \tilde{D}^2_{\nu_3}, \tag{17}$$

$$\text{IH}: \ \Delta m^2_{atm} = \kappa^2 \tilde{D}^2_{\nu_2}, \tag{18}$$

where NH(IH) represents the normal(inverted) hierarchy. The solar mass squared difference Δm^2_{sol} is given by

$$\text{NH}: \Delta m^2_{\text{sol}} = \kappa^2 \tilde{D}^2_{\nu_2}, \tag{19}$$

$$\text{IH}: \ \Delta m^2_{\text{sol}} = \kappa^2 (\tilde{D}^2_{\nu_2} - \tilde{D}^2_{\nu_1}). \tag{20}$$

The effective mass for neutrinoless double beta decay is given by

1) In general, the loop function also depends on the masses of charged leptons. However, we assume these masses to be negligible compared to the exotic particles inside the loop.

$$\mathrm{NH}: \langle m_{ee}\rangle = \kappa\left|+\tilde{D}_{\nu_2} s_{12}^2 c_{13}^2 e^{i\alpha_{21}} + \tilde{D}_{\nu_3} s_{13}^2 e^{-2i\delta_{CP}}\right|, \tag{21}$$

$$\mathrm{IH}: \langle m_{ee}\rangle = \kappa\left|\tilde{D}_{\nu_1} c_{12}^2 c_{13}^2 + \tilde{D}_{\nu_2} s_{12}^2 c_{13}^2 e^{i\alpha_{21}}\right|, \tag{22}$$

where the Majorana phase is defined by $\mathrm{diag}[1, e^{i\alpha_{21}/2}, 1]$ and we adopt the standard parametrization for the PMNS unitary matrix. The current KamLAND-Zen data [16] provide measured observables, and their upper bound is given by $\langle m_{ee}\rangle < (28-122)$ meV at a 90% confidence level. The minimal cosmological model ΛCDM $+\sum D_\nu$ provides an upper bound on $\sum D_\nu \leq 120$ meV [17, 18]. Moreover, the recent combination of DESI and CMB data gives a more stringent upper bound on this bound; $\sum D_\nu \leq 72$ meV [19].

E. Lepton-flavor violations and muon anomalous magnetic moment

$\ell_\alpha \to \ell_\beta\gamma$ process: First of all, let us consider the processes $\ell_\alpha \to \ell_\beta\gamma$ at one-loop level [1)]. The formula for the branching ratio can generally be written as

$$\mathrm{BR}(\ell_\alpha \to \ell_\beta\gamma) = \frac{48\pi^3 C_{\alpha\beta}\alpha_{\rm em}}{G_{\rm F}^2 m_\alpha^2}\left(|(a_R)_{\alpha\beta}|^2 + |(a_L)_{\alpha\beta}|^2\right), \tag{23}$$

where $\alpha_{\rm em} \approx 1/137$ is the fine-structure constant, $C_{\alpha\beta} \approx (1, 0.1784, 0.1736)$ for $((\alpha,\beta) = (\mu,e), (\tau,e), (\tau,\mu))$, $G_{\rm F} \approx 1.17\times10^{-5}$ GeV^{-2} is the Fermi constant, and $a_{L/R}$ is given by

$$(a_R)_{\alpha\beta} \approx \frac{1}{(4\pi)^2}\sum_{a=e,\mu,\tau}\sum_{i=1}^{3}\left(a_\nu^2 \frac{H_{\beta i}H_{i\alpha}^\dagger}{12 m_{S_1}^2} m_{\ell_\alpha} + b_\nu^2 \frac{Y_{\beta i}^* Y_{i\alpha}^T}{m_{S_2}^2} m_{\ell_\beta} F_I\left[\frac{D_{N_i}^2}{m_{S_2}^2}\right]\right), \tag{24}$$

$$(a_L)_{\alpha\beta} = \frac{1}{(4\pi)^2}\sum_{a=e,\mu,\tau}\sum_{i=1}^{3}\left(a_\nu^2 \frac{H_{\beta i}H_{i\alpha}^\dagger}{12 m_{S_1}^2} m_{\ell_\beta} + b_\nu^2 \frac{Y_{\beta i}^* Y_{i\alpha}^T}{m_{S_2}^2} m_{\ell_\alpha} F_I\left[\frac{D_{N_i}^2}{m_{S_2}^2}\right]\right), \tag{25}$$

where

$$F_I(x) = \frac{1-6x+3x^2+2x^3-6x^2\ln[x]}{6(1-x)^4}. \tag{26}$$

By assuming that $m_{\ell_\alpha} \gg m_{\ell_\beta}$, the formula can be simplified to

$$\mathrm{BR}(\ell_\alpha \to \ell_\beta\gamma) \approx \frac{48\pi^3 C_{\alpha\beta}\alpha_{\rm em}}{G_{\rm F}^2(4\pi)^4}\left[\frac{a_\nu^4}{144 m_{S_1}^4}\left|\sum_{a=e,\mu,\tau} H_{\beta a}H_{a\alpha}^\dagger\right|^2 + \frac{b_\nu^4}{m_{S_2}^4}\left|\sum_{i=1}^{3} Y_{\beta i}^* Y_{i\alpha}^T F_I\left[\frac{D_{N_i}^2}{m_{S_2}^2}\right]\right|^2\right]. \tag{27}$$

The formula for the muon $g-2$ can be written in terms of a_L and a_R and simplified as follows:

$$\Delta a_\mu \approx -m_\mu(a_R + a_L)_{\mu\mu} \approx -\frac{m_\mu^2}{(4\pi)^2}\sum_{a=e,\mu,\tau}\sum_{i=1}^{3}\left(a_\nu^2 \frac{H_{\mu a}H_{a\mu}^\dagger}{6 m_{S_1}^2} + 2b_\nu^2 \frac{Y_{\mu i}^* Y_{i\mu}^T}{m_{S_2}^2} F_I\left[\frac{D_{N_i}^2}{m_{S_2}^2}\right]\right). \tag{28}$$

Notice here that this contribution to the muon $g-2$ is negative; however, it is negligible compared to the deviation in the experimental value $O(10^{-9})$ [22].

F. Lepton universality

Here, we employ only the results of lepton universality from a precursor work [23]; the results provide the upper bounds on coupling H in terms of m_{S_1} and a_ν. We summarize these results in Table 3.

G. Dark matter

Relic density: Our DM is identified as the lightest Majorana fermion N_1 where we denote N_1 as X hereafter and its mass is m_χ. In order to analyze it simpler, we impose the following condition, $1.2m_\chi \lesssim D_{N_2} \leq D_{N_3}$, in order to evade an effect of co-annihilation interactions for the relic density of DM. [2)] Under the condition, the dominant contribution to the relic density arises from Y. Then, the non-relativistic cross section is expanded by relative velocity $v_{\rm rel}^2$; $(\sigma v_{\rm rel}) \approx a_{\rm eff} + b_{\rm eff} v_{\rm rel}^2 + O(v_{\rm rel}^4)$ and found as follows:

$$(\sigma v_{\rm rel}) \approx \frac{m_\chi^2}{48\pi(m_{S_2}^2 + m_\chi^2)^4}(m_{S_2}^2 + 2m_{S_2}^2 m_\chi^2 + 3m_\chi^4) b_\nu^4 \sum_{a,b=1}^{3}|Y_{ai}^* Y_{1,b}^T|^2 v_{\rm rel}^2, \tag{29}$$

where we have neglected the masses of charged leptons. The above cross section suggests that it is p-wave dominant. The relic density is then given by

1) The experimental bounds are summarized in Table 2.

2) More detailed computations are found in [24, 25].

Table 2. Summary of the experimental bounds of the LFV processes $\ell_\alpha \to \ell_\beta\gamma$.

Process	(α,β)	Experimental bounds (90% CL)	References
$\mu^- \to e^-\gamma$	(μ,e)	$\mathrm{BR}(\mu\to e\gamma) < 4.2\times10^{-13}$	[20]
$\tau^- \to e^-\gamma$	(τ,e)	$\mathrm{BR}(\tau\to e\gamma) < 3.3\times10^{-8}$	[21]
$\tau^- \to \mu^-\gamma$	(τ,μ)	$\mathrm{BR}(\tau\to \mu\gamma) < 4.4\times10^{-8}$	[21]

Table 3. Summary of the lepton universality and the corresponding bounds on $f_{\alpha\beta}$.

Process	Experiments	Bound (90% CL)
Lepton/hadron universality	$\sum_{q=b,s,d}\lvert V_{uq}^{\rm exp}\rvert^2 = 0.9999\pm0.0006$:	$\lvert H_{e\mu}^\dagger\rvert^2 < 0.007\left(\frac{m_{S_1}}{a_\nu \mathrm{TeV}}\right)^2$
μ/e universality	$\frac{G_\mu^{\rm exp}}{G_e^{\rm exp}} = 1.0010\pm0.0009$	$\lVert H_{\mu\tau}^\dagger\rvert^2 - \lvert H_{e\tau}^\dagger\rvert^2 < 0.024\left(\frac{m_{S_1}}{a_\nu \mathrm{TeV}}\right)^2$
τ/μ universality	$\frac{G_\tau^{\rm exp}}{G_\mu^{\rm exp}} = 0.9998\pm0.0013$	$\lVert H_{e\tau}^\dagger\rvert^2 - \lvert H_{e\mu}^\dagger\rvert^2 < 0.035\left(\frac{m_{S_1}}{a_\nu \mathrm{TeV}}\right)^2$
τ/e universality	$\frac{G_\tau^{\rm exp}}{G_e^{\rm exp}} = 1.0034\pm0.0015$	$\lVert H_{\mu\tau}^\dagger\rvert^2 - \lvert H_{e\mu}^\dagger\rvert^2 < 0.04\left(\frac{m_{S_1}}{a_\nu \mathrm{TeV}}\right)^2$

$$\Omega h^2 \approx \frac{1.07\times10^9}{\mathrm{GeV}}\frac{x_f^2}{3\sqrt{g^*}M_P b_{\rm eff}}, \tag{30}$$

where $g^*\approx100$, $M_P\approx1.22\times10^{19}$GeV, $x_f\approx20$. In our numerical analysis, we use a rather relaxed experimental range $0.11\le\Omega h^2\le0.13$ because we simplify our analysis of the relic density.

III. NUMERICAL ANALYSIS

In this section, we demonstrate numerical analyses based on all the experimental results that we have discussed. Then, we show the results of the LFVs, lepton $g-2$, and DM.

A. Numerical results of the lepton sector

First, we perform a χ square analysis adopting data from NuFit6.0 [15], where we use five reliable observables (three mixings, two mass square differences) for the analysis. The yellow points represent the interval of $2\sigma-3\sigma$, and the red ones $3\sigma-5\sigma$, where no solutions are obtained within 2σ. Our three input parameters are randomly selected within the following range:

$$\{\tilde{M}_2, |\tilde{c}_\nu|, |\tilde{d}_\nu|\} \in [10^{-5}, 10^5], \tag{31}$$

where we work on the fundamental region of τ, and $\tilde{c}_\nu, \tilde{d}_\nu$ are complex.

After the numerical analysis, we find that the IH case is not favored in the model, where the minimal χ^2 can be at most $O(1500)$. Thus, we summarize our results using only the NH case in the next subsection. Note that the parameters $\{a_e, a_\mu, a_\tau\}$ are chosen to fit the observed charged-lepton masses, and $\{a_\nu, b_\nu, M_1\}$ are related to fix the scale of the neutrino mass via κ, defined in Eq. (15). Thus, the relative neutrino mass and three mixing angles are fitted using the remaining parameters $\{\tau, c_\nu, d_\nu, M_2\}$ corresponding to seven real parameters. Three of these real parameters are related to complex phases; therefore, fitting the neutrino data is nontriavial. In fact, we would not be able to obtain any solutions in the IH case. To improve the fitting further, such as for IH, we need to change the assignment of the modular weight to increase the number of free parameters.

B. Neutrino observables in NH case

In Fig. 1, we show the allowed region of τ, and find that the allowed region is concentrated at nearby $|\mathrm{Re}[\tau]| = [0.0-0.2]$ and $\mathrm{Im}[\tau] = [1.26-1.28]$ where the value is close to the fixed point $\tau = i$. We also find a few points near the fixed point $\tau = \omega$. [1)]

In Fig. 2, we demonstrate the allowed regions for the absolute values (left) and argument ones (right) of $\tilde{d}_\nu$ and $\tilde{c}_\nu$ in NH. We show that the allowed region is at approximately $|\tilde{c}_\nu| = [10^{-4}-10^5]$ and $|\tilde{d}_\nu| = [10^{-5}-10^4]$, where $|\tilde{d}_\nu| \ll |\tilde{c}_\nu|$ is preferred, and $\mathrm{Arg}[\tilde{c}_\nu]$ and $\mathrm{Arg}[\tilde{d}_\nu]$ can be any value with little correlation.

In Fig. 3, we display the allowed region for $\delta_{\rm CP}$ deg (left) and $\langle m_{ee}\rangle$ meV (right) in terms of $\sum D_\nu$ meV. We show that most of the points are located at $|\delta_{\rm CP}| = [90-200]$ deg and few points are at approximately $\delta_{\rm CP} = [40-60]$ deg, and $\langle m_{ee}\rangle \approx [1-4]$ meV. The vertical magenta dotted line is the upper bound of the results of Planck+DESI [19] $\sum D_\nu \le 72$ meV, and the $\sum D_\nu$ range of our model is $[58-60]$ meV, which is a trivial consequence of two nonzero mass eigenvalues of active neutrinos.

In Fig. 4, we show the allowed region for $\langle m_{ee}\rangle$ meV

1) Note here that these points are not sufficiently close to the fixed points to investigate the mass matrices analytically by expanding modular forms in terms of deviation from the fixed points. To achieve such analysis, the absolute distance from the fixed points should be within 0.05.

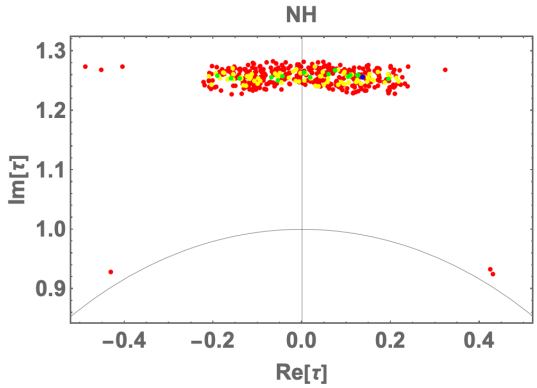

Fig. 1. (color online) Allowed region for real τ and imaginary τ in NH.

(left) and α_{21} deg (right) in terms of $\delta_{\rm CP}$ deg in NH. We show that the allowed region of α_{21} is concentrated at approximately [80 – 270] deg with few points outside the region.

We show a benchmark point (BP) that has the minimum $\Delta\chi^2$ in Table 4 and this BP will be employed to analyze the LFV, $g-2$, and DM in the next subsection.

C. Numerical results of LFVs, lepton $g-2$, and DM based on the neutrino results

Before our numerical analysis, we present some definitions. The neutrino-mass matrix does not depend on all the masses inside the loop, but the chi square analysis of the neutrino-oscillation data provides the value of κ. Their masses inside the loop determine the values of the LFVs, muon $g-2$, and relic density of DM. Thus, we rewrite Eq. (15) as follows:

$$\lambda_0 = -\frac{(4\pi)^6}{(a_\nu b_\nu)^2}\left(\frac{\kappa M_1}{m_\tau^2}\right). \tag{32}$$

When a_ν, b_ν, and M_1 are numerically fixed, λ_0 is numerically determined. Then, we impose the perturbative limit in our numerical analysis to be

$$\lambda_0 \lesssim \sqrt{4\pi}. \tag{33}$$

In addition, we restrict ourselves to the following conditions to forbid co-annihilation processes and obtain the mass-independent loop function of the neutrino-mass

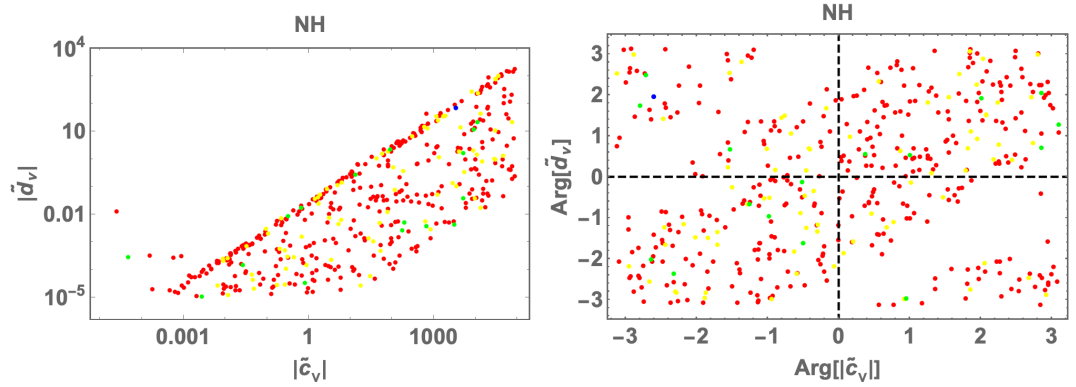

Fig. 2. (color online) Allowed regions for absolute values (left) and argument ones (right) of $\tilde{d}_\nu$ and $\tilde{c}_\nu$ in NH.

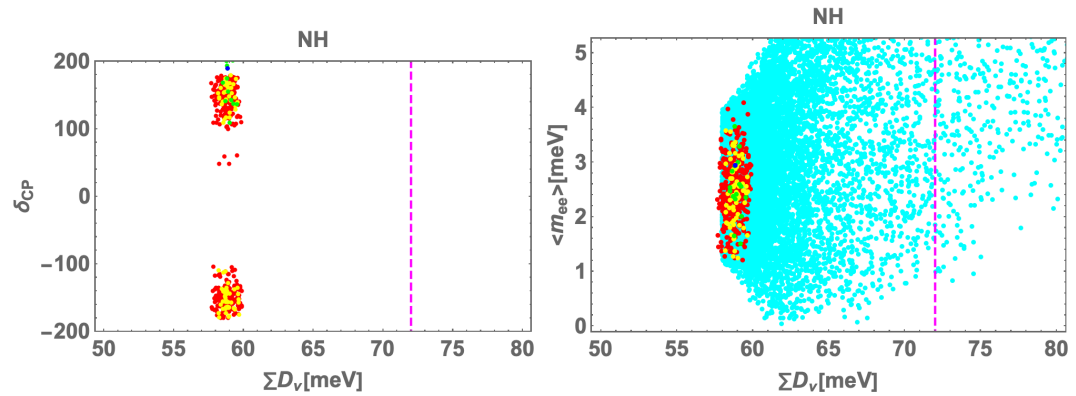

Fig. 3. (color online) Allowed regions for $\delta_{\rm CP}$ deg (left) and $\langle m_{ee}\rangle$ meV (right) in terms of $\sum D_\nu$ meV in NH. The vertical magenta dotted line is the upper bound of the results of Planck+DESI [19], $\sum D_\nu \leq 72$ meV. The cyan region in the left panel indicates the allowed region based on the experimental results of Nufit 6.0.

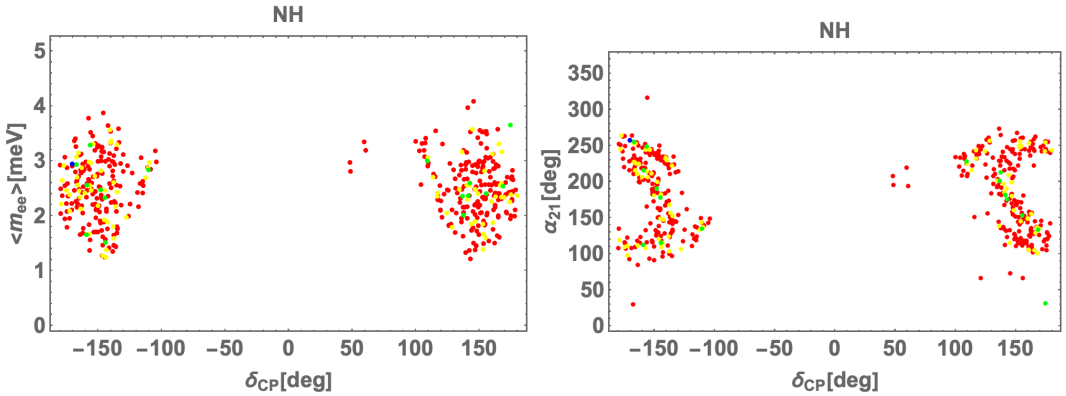

Fig. 4. (color online) Allowed region for $\langle m_{ee}\rangle$ meV (left) and δ_{CP} deg (right) in terms of δ_{CP} deg in NH.

Table 4. Numerical benchmark point (BP) of our input parameters and observables in NH. Here, this BP takes $\sqrt{\Delta\chi^2}$ as the minimum.

	NH
τ	$0.137+1.26i$
$\tilde{M}_2$	5.34×10^{-4}
$\tilde{c}_\nu$	$-2.85\times10^3-1.69\times10^3 i$
$\tilde{d}_\nu$	$-26.3+64.5i$
$[a_e,a_\mu,a_\tau]$	$[7.21\times10^{-6},-0.00139,0.0206]$
$\Delta m^2_{\rm atm}$	$2.51\times10^{-3}\text{eV}^2$
$\Delta m^2_{\rm sol}$	$7.56\times10^{-5}\text{eV}^2$
$\sin\theta_{12}$	0.553
$\sin\theta_{23}$	0.683
$\sin\theta_{13}$	0.147
$[\delta^\ell_{\rm CP},\ \alpha_{21}]$	$[-170°, 257°]$
$\sum m_i$	58.8 meV
$\langle m_{ee}\rangle$	2.94 meV
κ	3.49×10^{-14}
$\sqrt{\Delta\chi^2}$	2.24

matrix:

$$1.2m_\chi \le D_{N_2} \le D_{N_3}, \tag{34}$$

$$\epsilon_3 \le \frac{1}{5}, \quad 0.9m_{S_1} \le m_{S_2} \le 1.1m_{S_1}, \tag{35}$$

where we have defined ϵ_3 to be $\dfrac{D_{N_3}}{m_{S_1}}$.

Our input parameters are randomly selected from the following range:

$$\{a_\nu,b_\nu\} \in [0,\sqrt{4\pi}], \quad M_1/\text{GeV} \in [10^{-5},10^5], \tag{36}$$

where a_ν, b_ν are real and the other required parameters are employed by the BP in the previous section.

Our numerical analysis showed that Yukawa coupling $|b_\nu \times Y|$ exceeds the perturbative limit $\sim 4\pi$ to obtain the observed relic density of DM while satisfying the constraints of LFVs and lepton universalities. The correct relic density requires $O(100) \lesssim \text{Max}[|b_\nu \times Y|]$ for the NH case, applying allowed parameters that can fit the neutrino data. This implies that co-annihilations do not help to reduce the Yukawa couplings to the perturbative limit. We may move to one of the next minimum models by changing the modular weight of N_R to –2 instead of 0 to obtain one more mass parameter. This provides a wider region of allowed parameters, where the other assignments are the same as our model. However, we would still encounter difficulty in realizing the correct relic density while keeping the perturbative limit for the Yukawa couplings. This is because the DM annihilation cross section, Eq. (29), is p-wave dominant and we need a relatively larger coupling constant than that of the s-wave case. In addition, neutrino data and LFV constraints require heavy DM and new scalars that also suppress the DM annihilation cross section. Thus, obtaining the correct relic density in our minimal setting is difficult, and some extension is necessary.

If we do not satisfy the observed relic density and we perform our numerical analysis under the perturbative limit, we obtain the tendencies for electron $g-2$, muon $g-2$, and LFVs, as shown in Fig. 5. These figures suggests that $-\Delta a_e$ and $-\Delta a_\mu$ are at most 10^{-20} and 10^{-15}, respectively. However, LFVs, especially the $\mu \to e\gamma$ branching ratio, would be testable in the near future because its maximum value is close to the experimental limit.

D. Minimal extension to accommodate relic density of DM

We briefly illustrate one of the simplest solutions to explain the observed relic density without breaking our predictions for the neutrino sector, making use of a new

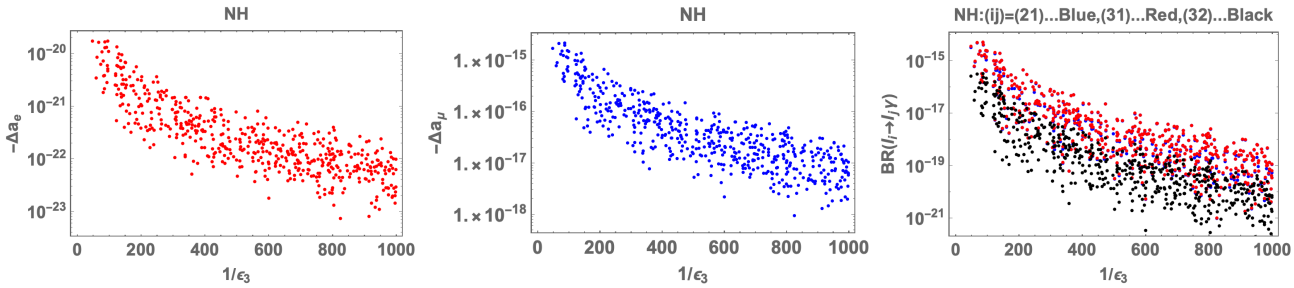

Fig. 5. (color online) Allowed region for electron $g-2$ (left), muon $g-2$ (center), and LFVs (right), where these points do not satisfy the observed relic density.

interaction. We introduce a singlet scalar boson S_0 that leads to new interactions

$$\mathcal{L}_{\rm new} = y_S S_0 \overline{N_R^C} N_R + \lambda_{\rm mix} S_0 H^\dagger H + \cdots, \tag{37}$$

where its modular weight is assigned to zero for simplicity, assuming it is a singlet under the A_4 symmetry, and we omit terms with $S^{\pm}_{1,2}$. We then have a Higgs portal to the SM by mixing between S^0 and h induced by the last term of $\mathcal{L}_{\rm new}$. Note that the addition of these interactions do not modify the neutrino mass, and the predictions in our analysis will not change.

As a result we have additional DM annihilation processes such as $\chi\chi \to S^0 \to f_{\rm SM} f_{\rm SM}$ and $\chi\chi \to S_0 S_0$. In particular, the s-channel cross section is useful for explaining the relic density because the annihilation cross section is enhanced nearby at $m_\chi \approx m_{S_0}/2$, where m_{S_0} is the mass of S_0. The annihilation cross section of the $\chi\chi \to S^0 \to f_{\rm SM} f_{\rm SM}$ process is approximately given by

$$(\sigma v_{\rm rel}) \simeq \frac{y_S^2 y_f^2 \sin^2\alpha}{2\pi} \frac{m_\chi^2}{(4m_\chi^2 - m_{S_0}^2)^2}, \tag{38}$$

where y_f is the SM Yukawa coupling for fermion f and $\sin\alpha$ indicates the Higgs-S_0 mixing. The relic density of DM is estimated as $\Omega h^2 \sim 0.1\ {\rm pb}/(\sigma v_{\rm rel})$, and we obtain

$$\Omega h^2 \sim 0.12 \left(\frac{m_\chi}{1\ {\rm TeV}}\right)^2 \frac{0.0081}{y_S^2 \sin^2\alpha} \left(1 - \frac{m_S^2}{4m_\chi^2}\right)^{-2}, \tag{39}$$

where we consider the top quark as f for simplicity. Thus, we can realize $\Omega h^2 \sim 0.12$ with $m_\chi = 1$ TeV, $y_S = 1$, and $\sin\alpha \sim 0.1$, even if we do not have resonant enhancement. With the resonant effect, we can fit the relic density for the small Higgs-mixing case without conflicting constraints of direct detection searches [26].

IV. CONCLUSIONS AND DISCUSSIONS

We investigated a three-loop induced neutrino mass model in a non-holomorphic modular flavor symmetry. We observed that some predictions in a framework that masses inside the loop do not depend on the structure of the neutrino mass matrix. Because our model has a rank two Yukawa matrix in the neutrino sector, the lightest neutrino-mass eigenvalue vanishes. Here, we realized a model with minimum free parameters, three complexes τ, $\tilde{c}_\nu$, $\tilde{d}_\nu$ and five reals a_e, a_μ, a_τ, $\tilde{M}_2$, κ, due to the appropriate charge assignments under the modular symmetry. Then, we performed chi-square analyses considering the neutrino-oscillation data. In particular, we observed rather narrow arrowed regions for the NH case, and we could not fit the data in the IH case. By adopting the best-fit value for NH, we further analyzed the lepton-flavor violation, muon $g-2$, lepton-flavor universalities, and DM. We have neglected all the complicated processes such as co-annihilation interactions by controlling the related masses. The numerical analyses showed that explaining the observed relic density within the perturbative limit is difficult. However, resolving this is easy by introducing a singlet boson without changing predictions in the neutrino sector.

APPENDIX A: LOOP FUNCTION

The loop function at the third level is generally obtained only via numerical methods. However, if some conditions are imposed, one can analytically integrate it out. Here, we show the integration under the case of $D_{N_i} \ll m_{S_{1,2}}$, to which we apply our model, where $m_{S_1}^2 = m_{S_2}^2 \pm \delta m_S^2$ with $\epsilon_S \equiv \dfrac{\delta m_S}{m_{S_2}} \ll 1$.

One can expand the integration in terms of $\epsilon_i (\equiv D_{N_i}/m_{S_1})$ and ϵ_S as follows:

$$F \approx a_0 + a_1 \epsilon_i^2 + b_1 \epsilon_S^2 + O(\epsilon_i^4) + O(\epsilon_S^4), \tag{A1}$$

$$a_0 \approx \int [{\rm d}x]_3 \int [{\rm d}x']_3 \int [{\rm d}x'']_3 \left[\frac{1}{\dfrac{y''(y+z)}{(1-z)z} + \dfrac{z''(y'+z')}{(1-z')z'}} \right], \tag{A2}$$

$$a_1 \approx -\int [\mathrm{d}x]_3 \int [\mathrm{d}x']_3 \int [\mathrm{d}x'']_3 \left[\frac{x''}{\left(\frac{y''(y+z)}{(1-z)z} + \frac{z''(y'+z')}{(1-z')z'} \right)^2} \right], \tag{A3}$$

$$b_1 \approx \int [\mathrm{d}x]_3 \int [\mathrm{d}x']_3 \int [\mathrm{d}x'']_3 \left[\frac{(-1+z)z(-1+z')z'(-yy''z' + yy''z'^2 - y'zz'' + y'z^2z'')}{(-yy''z' - y''zz' + yy''z'^2 + y''zz'^2 - y'zz'' + y'z^2z'' - zz'z'' + z^2z'z'')^2} \right], \tag{A4}$$

where $a_0 \approx 0.062$, $a_1 \approx -2.92$, $b_1 \approx -0.0281$, and $\int [\mathrm{d}x]_3 \equiv \int_0^1 \mathrm{d}x \int_0^{1-x} \mathrm{d}y|_{z=1-x-y}$.

References

[1] B. Y. Qu and G. J. Ding, JHEP **08**, 136 (2024), arXiv: 2406.02527
[2] G. J. Ding, J. N. Lu, S. T. Petcov *et al*., (2024), arXiv: 2408.15988
[3] C. C. Li, J. N. Lu, and G. J. Ding, JHEP **12**, 189 (2024), arXiv: 2410.24103
[4] T. Nomura and H. Okada, (2024), arXiv: 2408.01143
[5] T. Nomura, H. Okada, and O. Popov, Phys. Lett. B **860**, 139171 (2025), arXiv: 2409.12547
[6] T. Nomura and H. Okada, (2024), arXiv: 2412.18095
[7] B. Y. Qu, J. N. Lu, and G. J. Ding, (2025), arXiv: 2506.19822
[8] H. Okada and Y. Orikasa, (2025), arXiv: 2501.15748
[9] T. Kobayashi, H. Okada, and Y. Orikasa, (2025), arXiv: 2502.12662
[10] M. A. Loualidi, M. Miskaoui, and S. Nasri, (2025), arXiv: 2503.12594
[11] T. Nomura, H. Okada, and X. Y. Wang, (2025), arXiv: 2504.21404
[12] M. Abbas, PHEP **2025**, 7 (2025)
[13] E. Ma, Phys. Rev. D **73**, 077301 (2006), arXiv: hep-ph/0601225
[14] L. M. Krauss, S. Nasri, and M. Trodden, Phys. Rev. D **67**, 085002 (2003), arXiv: hep-ph/0210389
[15] I. Esteban, M. C. Gonzalez-Garcia, M. Maltoni *et al*., JHEP **12**, 216 (2024), arXiv: 2410.05380
[16] S. Abe *et al*. (KamLAND-Zen), (2024), arXiv: 2406.11438
[17] S. Vagnozzi, E. Giusarma, O. Mena *et al*., Phys. Rev. D **96**, 123503 (2017), arXiv: 1701.08172
[18] N. Aghanim *et al*. (Planck), Astron. Astrophys. **641**, A6 (2020) [Erratum: Astron. Astrophys. **652**, C4 (2021)], arXiv: 1807.06209
[19] A. G. Adame *et al*. (DESI), (2024), arXiv: 2404.03002
[20] A. M. Baldini *et al*. (MEG), Eur. Phys. J. C **76**, 434 (2016), arXiv: 1605.05081
[21] J. Adam *et al*. (MEG), Phys. Rev. Lett. **110**, 201801 (2013), arXiv: 1303.0754
[22] G. W. Bennett *et al*. (Muon g-2), Phys. Rev. D **73**, 072003 (2006), arXiv: hep-ex/0602035
[23] J. Herrero-Garcia, M. Nebot, N. Rius *et al*., Nucl. Phys. B **885**, 542 (2014), arXiv: 1402.4491
[24] A. Ahriche and S. Nasri, JCAP **07**, 035 (2013), arXiv: 1304.2055
[25] K. Cheung, H. Ishida, and H. Okada, (2016), arXiv: 1609.06231
[26] S. Kanemura, S. Matsumoto, T. Nabeshima *et al*., Phys. Rev. D **82**, 055026 (2010), arXiv: 1005.5651